Optica Applicata, Vol. XXXII, No. 4, 2002

Advances of optical sensors in biomedicine

UWE BINDIG

Laser- und Medizin-Technologie GmbH Berlin, Fabeckstr. 60–62, 14195 Berlin, Germany.

EWA ROHDE, GERHARD MÜLLER

Laser- und Medizin-Technologie GmbH Berlin, Fabeckstr. 60–62, 14195 Berlin, Germany.

Benjamin Franklin University Hospital, Freie Universität Berlin, Department of Medical Physics and Laser Medicine, Fabeckstr. 60–62, 14195 Berlin, Germany.

Analytical techniques based on sensors for medicine require direct measurements (either non-invasive or minimally invasive ones) which must be robust, reliable, safe and fast. The most frequently used techniques in this respect are optical methods. Recent developments in optics and optoelectronics provide powerful means for innovations in technology, especially in biomedical sciences. Optical techniques and sensor devices will foster non-invasive or minimally invasive medical procedures in diagnostics and therapy. One of the extensively growing fields is laser medicine, including such areas as infrared as well as fluorescence spectroscopy for tissue diagnostics and the visible and near infrared range, *i.e.*, for on-line quality control of human blood or blood products. For the diagnostics of infectious diseases ion-mobility spectroscopy can be used for future applications in monitoring or safety control. The use of optoelectronics can also play an important role in technological processes of food production and in controlling the final products. Therefore, appropriate sensors and methodologies must be developed. The applicability of optical and fiber-optical methods and some non-optical methods is discussed, with due consideration to characterization and monitoring in biomedicinal diagnostics.

1. Introduction

Analytical techniques based on sensors for medicine require direct measurements (either non-invasive or minimally invasive ones) which must be robust, reliable, safe and fast. The most frequently used techniques in this respect are optical methods. The applicability of optical and fiberoptical methods and some non-optical methods is discussed, with due consideration to characterization and monitoring in biomedicinal diagnostics.

For this purpose, various wavelength ranges can be used. Detection of non-fluorescent bio-markers is possible in the UV/VIS range, whereas due to an enhanced signal-to-noise ratio bio-fluorophores, *e.g.*, porphyrine, flavine or β-Nicotinamide adenine dinucleotide (NADH), will be determined by sensitive fluorescence techniques. Vibrational spectroscopy (infrared and Raman) which is between the

visible and microwave ranges of the electromagnetic spectrum, can even be used for medical diagnostics. Bearing in mind that normal biological tissue is a non-transparent medium, any other scattered light measuring techniques could also be useful.

Other methods, such as ion mobility spectroscopy (IMS) or the matrix-assisted laser desorption or ionisation – time of flight (MALDI–TOF), are discussed in terms of feasibility and application.

2. Optical methods

2.1. Infrared spectrometry

Subdivided into the near, mid and far infrared (NIR, MIR, FIR), the infrared range lies between the visible and microwave range. An absorption takes place when the dipole moment is changed. Higher energetic modes of the vibrational transition state are reached by discrete absorptions (Fig. 1).

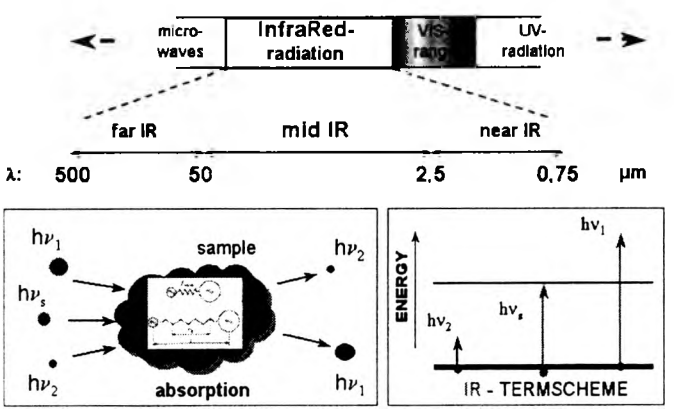

Fig. 1. Localization of the MIR range and a scheme for the IR absorption.

IR-spectroscopy is a non-destructive, rapid and sensitive optical method, which is mostly used for analytical purposes. In modern IR spectrometry the technical principle is based on the Michelson interferometer. By interaction of the IR radiation in the wavelength range 4000–800 cm^{-1} an IR spectrum can be recorded in a few milliseconds. This results in an interferogram which is converted to an absorption spectrum using Fourier transformation. Routine measurement modes are transmission, reflectance and attenuated total reflectance (ATR). The transmission mode is the most frequently used one. Elastic scattering is not possible above 2.5 μm due to the correlation particle size/wavelength. Absorption, elastic scattering and reflection (diffuse and specular) can be used in non-contact measuring modes, whereas ATR and fiber optic evanescent wave spectroscopy (FEWS) are used for measurements where the target is in direct contact with the fiber and crystal respectively, through which the IR radiation is transmitted. Examples for an IR fiber optical set-up and for an IR microscope are shown in Fig. 2. Maximal spatial resolution can be attained with an

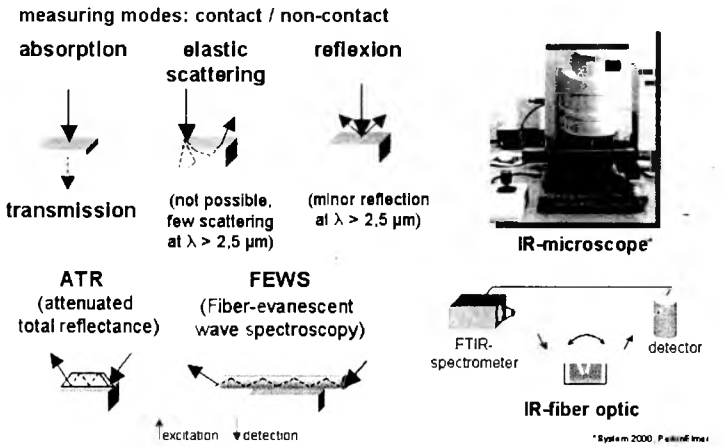

Fig. 2. View on popular IR measurement modes, a picture for an IR microscope and the IR fiberoptical set-up.

aperture of 10×10 µm^2 for IR microscopic measurements in transmission, ATR and remission mode.

Over the last decades the development and design of cylindrical optical fibers made of flexible quartz wave guides, paved the way for many new applications and new technologies in the medical field. For example, the development of laser assisted endoscopy in minimally invasive medicine is based on the application of efficient and powerful light guide systems [1]. Providing a useful technique for topical non-invasive medical diagnostics, flexible fibers contribute to minimizing patients' pain and overall cost reduction.

It is our aim to use IR spectroscopy as a tool for optical biopsy of human tissue for identification and differentiation, and in the future, as a new and sensitive method for tumour diagnostics. Figure 3 shows the IR transmission spectra of thin tissue sections from normal and tumours human colon specimens taken from the same study (spot

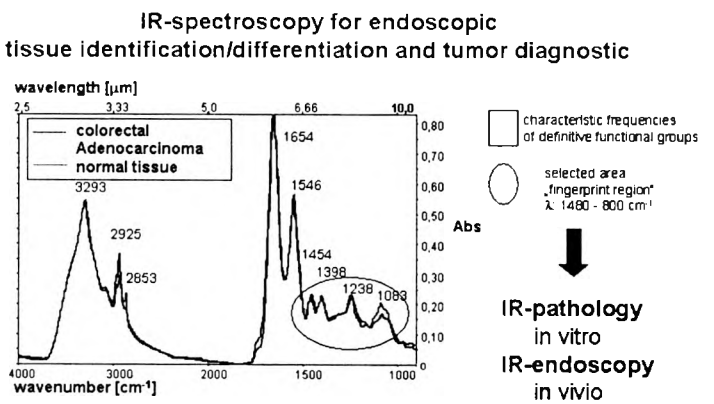

Fig. 3. IR transmission spectra from 10 µm thin sections of tumours and normal colonic tissue.

size 800×800 μm^2). There are only slight differences in their spectral characteristics. Due to a limited number of functional chemical groups there are regions of characteristic frequencies which can be assigned to distinct classes of bio-molecules, *e.g.*, lipids, proteins or carbohydrates. These regions are marked in the IR spectrum in Fig. 3. The region from 1500–800 cm^{-1} is called the "fingerprint region" and contains specific information. Our aim is to use the knowledge gained about the tissue-specific IR signature for IR pathology (*in vitro*) to enable the development of an IR endoscopic (*in vivo*) device.

The gold standard in histopathology is the sectioning of tissue samples (7–10 μm thin) preserved in formalin, which are then selectively stained. Hematoxylin and eosin is the most frequently used tissue staining method. When performed correctly, this method enables an experienced pathologist to evaluate pathological changes in the tissue according to the staining behavior and the colour intensity of the tissue components. Changes in the density of cell nucleus and the morphology of the tissue cells as well are an indication of a breakdown in the cyto-skeleton.

For the IR spectroscopic investigations, 10 μm thin tissue sections were cut from the native tissue without embedding materials being used. These sections were placed upon calcium fluoride slides and analyzed using IR microscopic standard procedures. For this purpose, IR maps were made in transmission mode at a resolution of 100×100 μm^2 in the wavelength range 4000–900 cm^{-1}. To improve the signal-to-noise ratio, 16 scans per pixel were added. The tissue was then stained and the tissue components assigned according to the standard procedure. This way, one defined IR spectrum could be assigned to each tissue component. Prior to this, the IR microscopic images of the native and the stained tissue sections had been compared to ensure both correct assignment and that the staining procedure had not caused any changes in the specimen by loss of tissue, cracks or shrinkage, *etc.* Such changes could falsify the results and give rise to misinterpretation. The development of IR reference spectra for

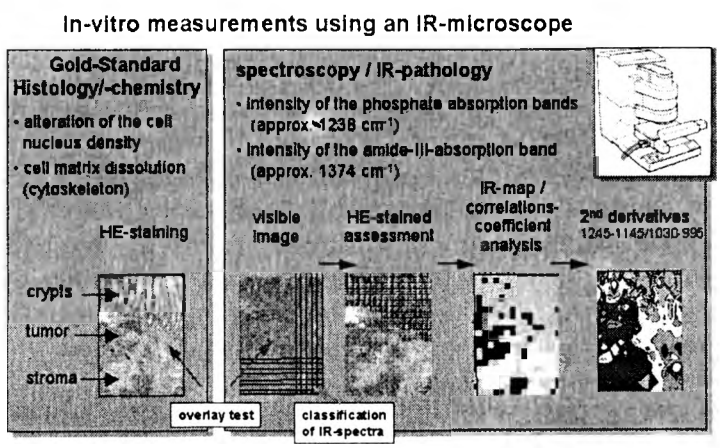

Fig.4. Comparison of the histo-pathologic *vs.* IR spectroscopic examination. The standard procedure for the IR mapping is shown.

the individual tissue components permitted a classification in the IR map by correlation coefficient analysis. In particular, spectral components, which are allocated to the range of phosphate vibrational bands and the amide-III absorption, correlate with the observed alterations in the histopathology. Whereas the phosphate vibrational band is related to the DNA/RNA content, which is represented by the cell nucleus density, the amide-III-band represents the marker for the lipid and protein content which relates to the cell morphology. However, in colonic tissue there are mucin secreting tumours. Mucin is a polysaccharide and can also be detected in the IR range of approximately imately 1000 cm^{-1}. To increase the process efficiency, an evaluation was made limiting the spectral range and using mathematical algorithms (Fig. 4). This evaluation proved to be successful [2]–[6].

Optical fibers transparent in the MIR make it possible to carry out absorption measurements at a remote location (Fig. 5). IR fibers can be used for measurements in the remission and ATR mode. If the IR fiber is in contact with a sample that has characteristic absorption lines, the total transmission of the fiber and sample will decrease at these lines. This can be utilized for determining the absorption of a sample in a non-destructive manner.

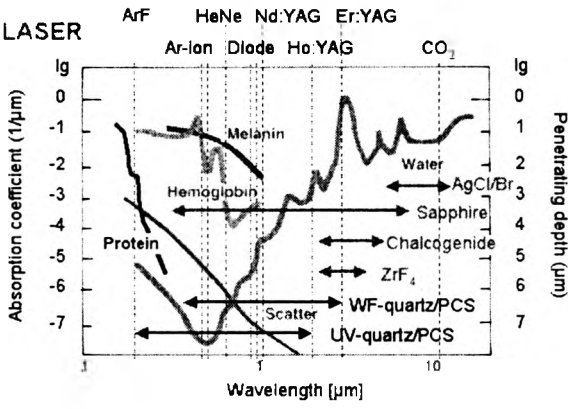

Fig. 5. Absorbance from certain biological compounds and the wavelength range for the transmittance from different waveguides.

It has been found that normal tissues exhibit absorption spectra different from diseased tissues, and it can be assumed that each diseased state of biological tissue has its own distinct characteristic IR spectral pattern [6]–[8]. However, marked differences can be found between the methods of sample preparation in terms of the measuring mode, the measured parameters and the conditions of the sample. In order to avoid artifacts to be caused by the sample preparation, fiber-optic methods are recommended. An IR fiber-optic sensor can be inserted through a biopsy needle or a catheter and measurements can be carried out in real-time. This will permit visible information and IR-spectroscopic data to be combined in both minimally invasive medicine (endoscopy) and open surgery.

In the MIR range polycrystalline silver halide fibers are preferred to chalcogenide or fluoride glass fibers, *e.g.*, Te-As-Se (TAS) wave guides [9], [10]. The former are particularly suitable because of their transparency in the infrared and their physical properties, namely they are non-toxic, flexible, non-hydroscopic, of low optical attenuation and have a long term stability. New techniques and modifications to the fiber type, material, geometry, shape and coating extend the range of applications, so that IR fibres can be used as biosensors [11]–[17]. This may be attractive because their use does not require any specific expert knowledge although they do provide accurate findings with samples that have not been treated at all or minimally, only.

Some possible applications in medicine and pharmaceutics have been published which are based on fiber-optic MIR spectrometry [18]–[20]. For example, KATZIR *et al.* [21] have designed a special measuring cell for an IR spectrometer which is equipped with a silver halide fiber to analyse blood serum; ARTJUSHENKO *et al.* [20] as well as BUTVINA *et al.* [22] have used IR fibers for the detection of melanoma and other skin diseases. This was also described by BRUCH *et al.* [23] where they have used the Fourier transform infrared evanescent wave spectroscopy for the spectral characterization. Acupuncture points on human skin were investigated too [24]. Attempts were made by WU *et al.* [25] using chalcogenide fiber-optic techniques to distinguish malignant from normal oral tissues and for diagnosis of cancer [25], [26]. Lead salt diode laser, which have been used a long time for gas analysis [27], [28], may enhance the sensitivity of detection for monitoring and diagnostics of tissue. Even the application of quantum cascade laser seems to be a new promising tool for the IR diagnostics.

Currently there is no routine clinical application which uses IR sensors. We have focused our attention on the biomedical application of IR spectroscopy for diagnostics purposes such as the detection of changes within biological tissues. This method may

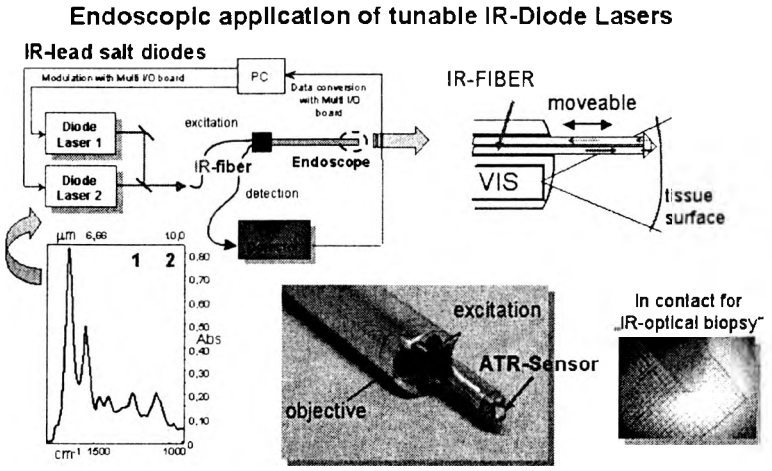

Fig. 6. Experimental set-up for IR fiber-optic measurements using IR laser diodes as excitation source and a prototype of an IR sensor which could be used for an IR endoscopic inspection.

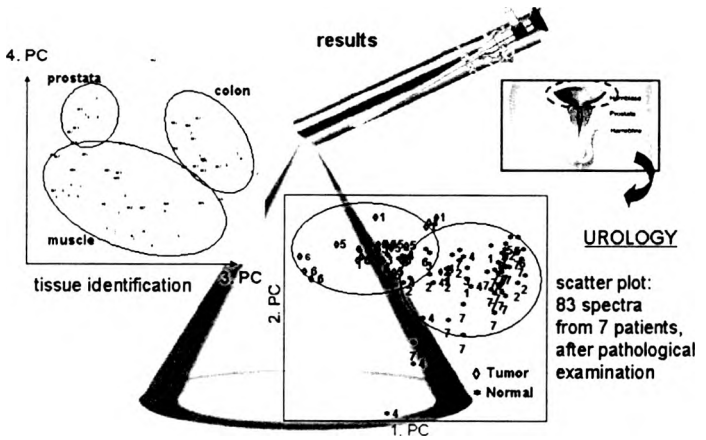

Fig. 7. Results for IR endoscopic measurements *in vitro*. Measurements were done either by using different non human tissue (bladder, colon, muscle) and for the identification of human bladder in order to differenciate normal and tumours tissue.

even be used for the real time monitoring of coagulation processes or on-line diagnosis of different bio-fluids.

A fiber-optic laboratory set-up for an IR endoscope was realised with multimode IR laser diodes which, contrary to commercial IR emitters, have a power range of 0.5–1 mW. These lead salt diodes can be controlled throughout the wavelength range via current and temperature. A diamond prism directly connected to the silver halide fibers serves as an ATR sensor face (Fig. 6). First investigations were made on non -human tissue. The scatter plot shows a differentiation of specific tissue types (bladder, muscle, colon) (Fig. 7). Investigations using human tissue provided by the urology department also showed a differentiation of tumours and non-tumours tissue [29].

2.2. NIR fluorescence

It is known that many investigations have been made on liquid samples in the field of NIR spectroscopy using molecule harmonic oscillations. The excellent correlation of the spectroscopic measuring data with the data determined by biochemical methods demonstrates the potential of this optical analysis procedure. Fluorescence optical procedures also proved to be very sensitive to the detection of bio-fluorophores when monitoring bio-processing and transformation (Fig. 8).

2.2.1. Auto-fluorescence for optical biopsy

Fluorescence diagnostics can be a tool to investigate metabolic behaviour of tissue, especially of tumours diseases [30]–[33]. So the cellular metabolism of infected *vs.* normal cells is significantly different, *e.g.*, by various amounts of coenzymes and perforants with respect to the tumour stage. The LENA (laser-induced endoscopic auto -fluorescence) fiber optic diagnostic system (see Fig. 9) is used for minimal invasive *in vivo* determination of the metabolic changes for the purpose of diagnostic tissue

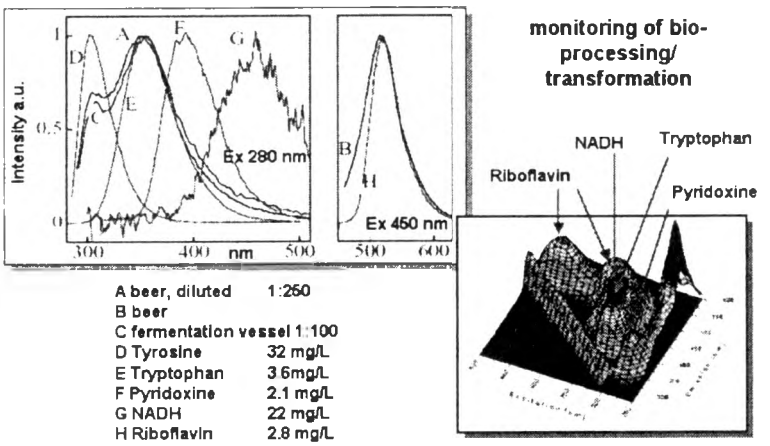

Fig. 8. Fluorescence spectra of bio-fluorophores for determination and monitoring.

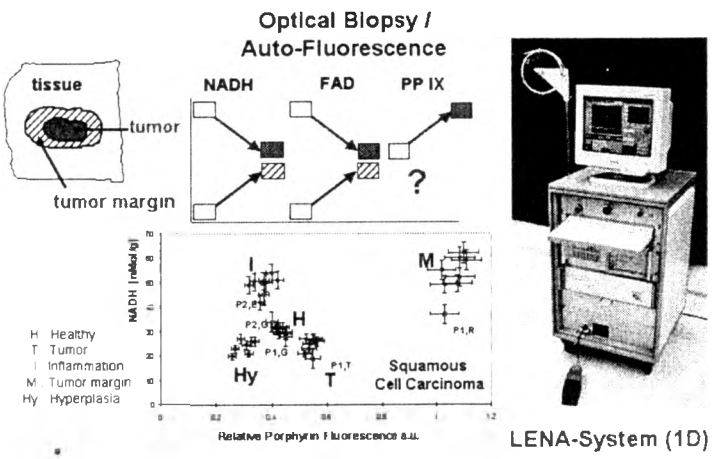

Fig. 9. LENA system.

differentiation. This is possible by combining the information of two fluorescence channels. By means of a NADH fluorescence signal, which is time domain measured and simultaneously rescaled (quantitatively in nMol/g), and a protoporphyrin IX (PP IX) fluorescence signal the following five histological conditions can be well discriminated in certain circumstances: healthy squamous ephithelium tissue, squamous cell carcinoma (margin), squamous cell carcinoma (center), inflammation and hyperplasia.

The individual histological conditions show differences in the NADH concentration, part of which are statistically significant (95% significance). In particular, the three conditions relevant for tumour diagnostics, healthy, tumour margin and tumour center, can be significantly discriminated from each other. Obviously, another parameter is required in order to discriminate a tumour border from

inflammatory processes and to isolate a tumour center from a hyperplasia. So the 2nd parameter is the relative PP IX fluorescence.

The system comprises two lasers, a short-pulsed nitrogen laser and a He-Ne laser. It is suitable for external body surfaces and endoscopically also for internal body surfaces and can be efficiently used for depths up to 200 μm.

The spectroscopic imaging system (SIMAS) is an imaging fluorescence diagnostic tool for experimental optical biopsy of tumours. For its application different metabolic processes of various histological conditions are utilized. The SIMAS leads itself to the detection of both NADH fluorescences and PP IX fluorescences. The SIMAS fluorescence diagnostic system consists of a central unit with integrated excitation light source (UV lamp), control unit for microchannel plate-supported camera and PC. The complete system is controlled via a graphics display. The SIMAS can be operated both in single-monitor and twin-monitor design. The second monitor serves as a physician's monitor permitting him to optimally examine the area to be investigated. The measuring process can be started either directly via the control unit or through the pedal switch.

The measuring head consists of a commercial-type Zeiss surgical microscope to which a sVHS camera for native images and a microchannel plate-supported camera for fluorescence images are fitted. An electronically controlled filter changer is used for selecting the fluorescence wavelengths. The system includes a mercury vapourizer that can be changed from white to UV and features an optical power output of 200 W. The excitation light is coupled into the measuring head through a liquid light guide. The RGB image is taken by a sVHS camera. The fluorescence light is taken by a microchannel plate-supported camera, the maximum sensitivity of which is 100 μLux.

Figure 10 shows the colour image of a tumour part of which is covered with fibrin. The dark contrast in the fluorescence image represents the blood crust (not shown). In the lower part of the picture there is a spot with heavy fluorescence. Tumour border, healthy tissue and fibrin cover cannot be clearly discriminated. Figure 10 even shows

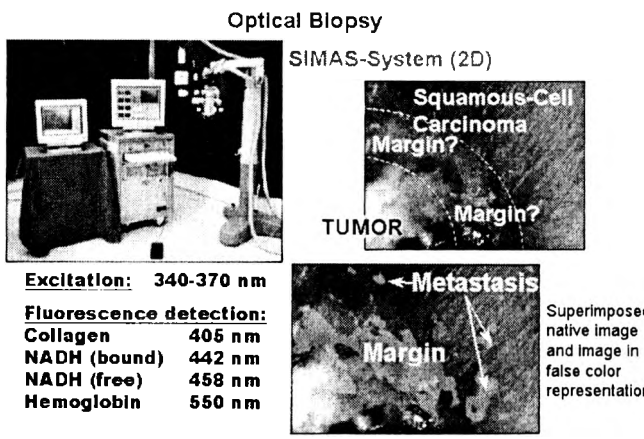

Fig. 10. SIMAS arrangement.

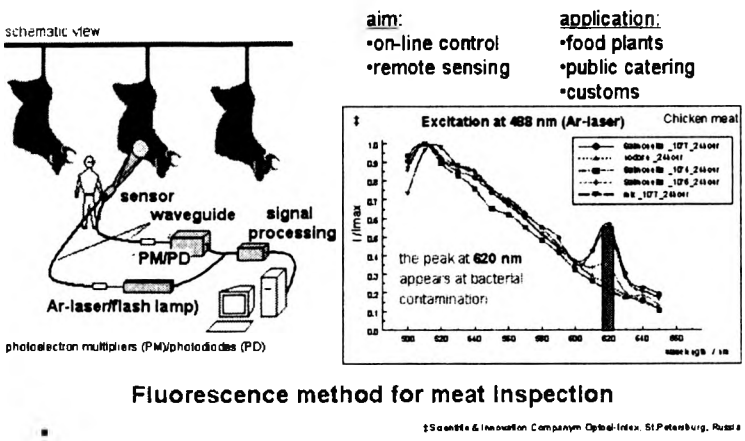

Fig. 11. Fiber-optical detection of bacterial contaminations by fluorescence spectroscopic methods.

the colour image which is superimposed by the false colour-coded fluorescence image. Both the tumour and the tumour border can be clearly discriminated from the healthy tissue.

According to statistics, only in North America alone nearly 7 million people a year suffer from diseases caused by bacteria infecting the food. In principle, the fluorescence method for the detection of bacterial contamination is based on transformation of the fluorescence spectrum of food stuff surface to be analyzed. For the non-contact check-up a fiber optic sensor could be the tool for the bacterial contamination diagnostics. So a simple fiber-assisted method can be applied, *e.g.*, to monitor bacterial contamination of meat products. This procedure was tested with the detection of salmonella contamination in meat. (Fig. 11). For the excitation either a laser or a xenon flash lamp can be employed for the selection of required spectral bands. Photodiodes or photomultipliers may be used for the spectral band selection.

2.2.2. Luminescence

A co-operative investigation was done for silicon-based biosensor that changes colour in the presence of different bio-organic relevant targets. Porous silicon formed from etching contains millions of tiny holes in the silicon-wafer. This structure provides a large surface area for contact with target molecules. By confirming the luminescence generated in the central layer of the microcavitiy, the photoluminescence spectrum is composed of multiple sharp and narrow peaks. Upon the refractive index change the photoluminescence spikes shift, thereby generating a detectable signal. In the first step, modifications of the internal porous silicon surface by different derivates of gluconamide were carried out in order to detect the enzyme concanavalin A (Fig. 12). Now success in determining Gram-negative bacteria was reported [34], [35]. The silicon surface was functionalized by a Lipid A binding receptor, which is responsible for Lipopolysaccharide (LPS). LPS is an endotoxin and is located on the outer bacterial cell membrane. A shift of 3–4 nm was observed when the sensor was exposed to a

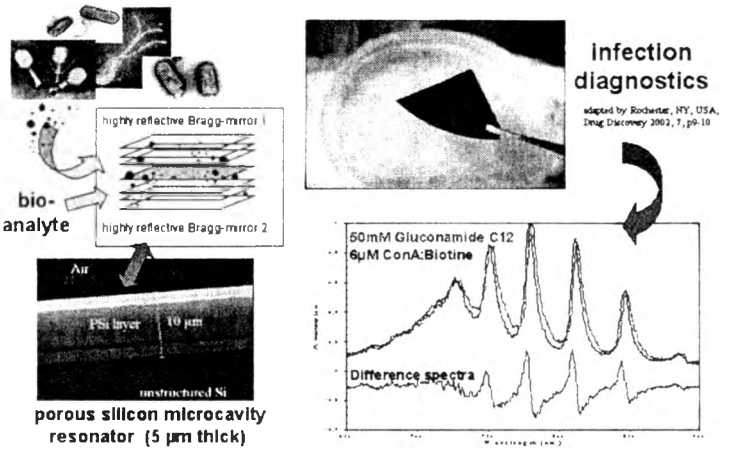

Fig. 12. Biosensor based on porous silicon for medical application.

lysed bacteria solution. However, a minimal amount of 1.7 µg bacteria could be detected. Due to the large three-dimensional internal surface structure, the porous sensor has a distinct enhanced sensitivity, compared to the common 2D-sensors with a clean 2D-surface.

2.2.3. Blood analysis

The most important bio-fluid in medicine is whole human blood. Until now there have been no objective, non-invasive procedures available for quality assurance and quality control of erythrocyte or thrombocyte concentrates. The situation is similar for heart -lung machines where there are no precision on-line monitoring processes available to determine hematocrit and blood oxygenation levels. Our efforts, therefore, are aimed at developing a portable on-line measuring system for heart-lung machines and an optical sensor system for checking blood bags. This requires exact knowledge of the physical parameters and remission with varying physiological data. Ideally these parameters should be directly available using a simple optical method. The optical parameters absorption coefficient μ_a, scattering coefficient μ_s and the anisotropy factor g were selected because blood is a strong absorbing and scattering medium. For the determination of the micro-optical parameters, the total transmission T, the diffuse transmission D and the diffuse remission R were established at an optimized Ulbricht sphere measuring set-up Lambda 900 (Perkin–Elmer) in a flow metering cuvette, specifically developed for this purpose. Data analyses were carried out, *i.e.*, by partial least square and principal component analysis.

Simulation calculations enabled us to show that for defined blood parameters wavelength ranges can be found which are characterized by at least one significantly dependent microoptical parameter. The macrooptical parameters within the wavelength range from 250 to 850 nm were measured under flow conditions on human blood using erythrocyte concentrates. The interdependence of the physiological blood

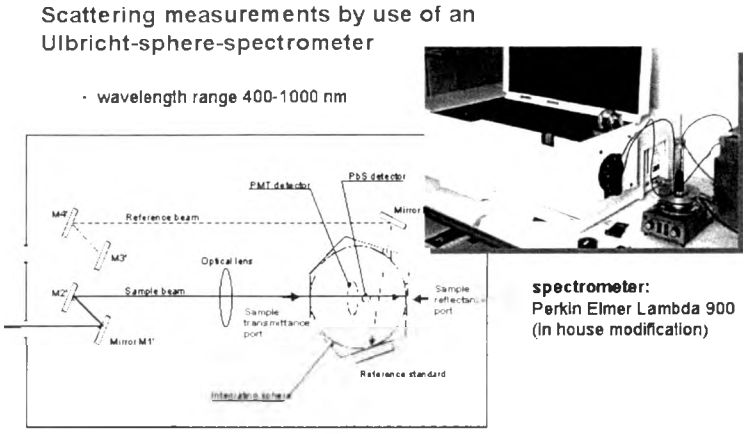

Fig. 13. Modified laboratory device for the determination of optical blood parameter.

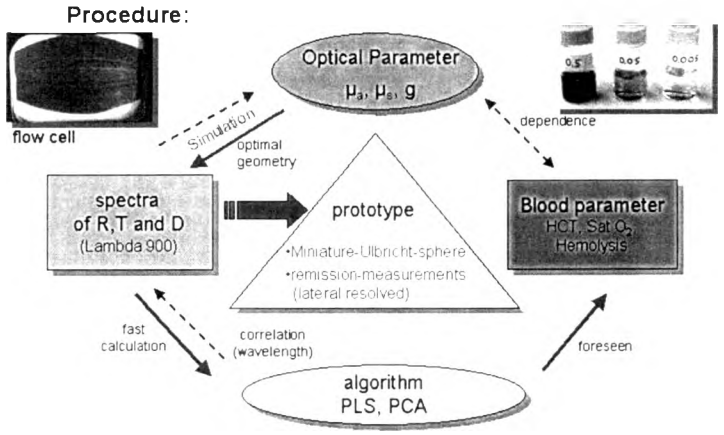

Fig. 14. Survey concerning the procedure to determine blood parameters.

parameters hemolysis degree, plasma osmolarity, shear rate of the flowing blood and degree of oxygenisation were recorded. A specific blood reservoir was developed to avoid any sedimentation effects and to permit continuous filtering and supply with a 95% nitrogen and 5% oxygen gas mixture (Figs. 13, 14). According to Fig. 15, the effects of the hemolysis differ considerably within the 3 optical parameters. At 660 nm total remission decreases slightly with increasing hemolysis, then it remains constant, while the total transmission initially increases to about 40% and then remains almost constant with increasing hemolysis. In contrast, the diffuse transmission remains almost unchanged at 40% hemolysis, but drops exponentially to zero at 100% hemolysis. This is due to an almost complete neutralization of the scattering effect at full hemolysis and shows that hemoglobin, with a refractive index above that of the surrounding medium, is almost exclusively responsible for the scattering properties. A prototype mobile blood bag measuring system was designed (Fig. 16), based on

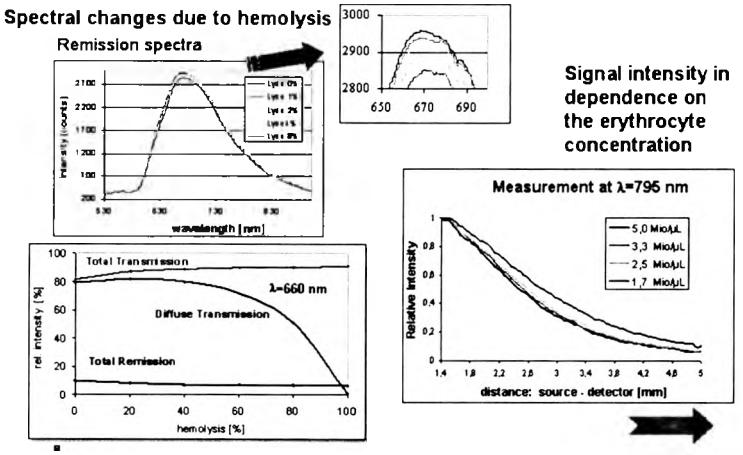

Fig. 15. NIR spectra due to the hemolysis of blood.

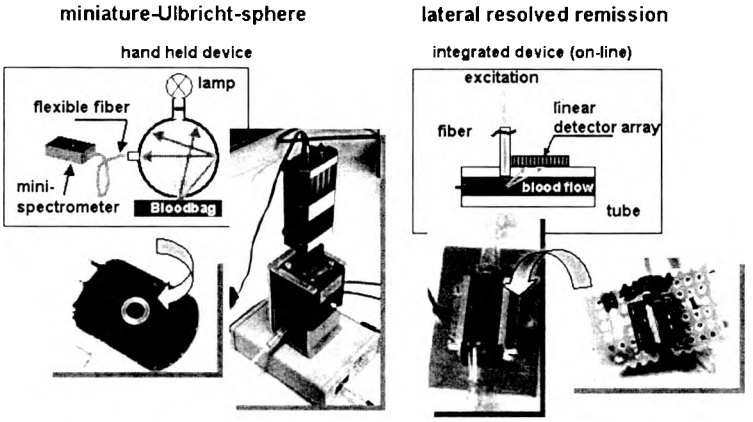

Fig. 16. Picture of prototypes, which may be used for the quality control of blood and related products.

these and other results. Simulation results indicate that measuring the lateral scattered light profile may also be an efficient method for the determination of blood parameters. First results with a cuvette (wall thickness 1 mm) showed a significant dependence on the erythrocyte concentration from the half-width value of the measuring signal (Fig. 15). The measuring set-up designed includes two diode lasers in the 650–800 nm range as light source (Fig. 16) [36]–[40].

The membranes of red blood cells are covered with different kinds of proteins determining decisively the aggregation and disaggregation properties of erythrocytes. Linear aggregates of different lengths are formed. End-to-side connections turn them into a 3D-network (clumps) which influences the rheological properties of the blood sample (Fig. 17). Morbid changes in the human body are reflected by changes in the kind and concentration of these proteins and consequently modify the aggregation and

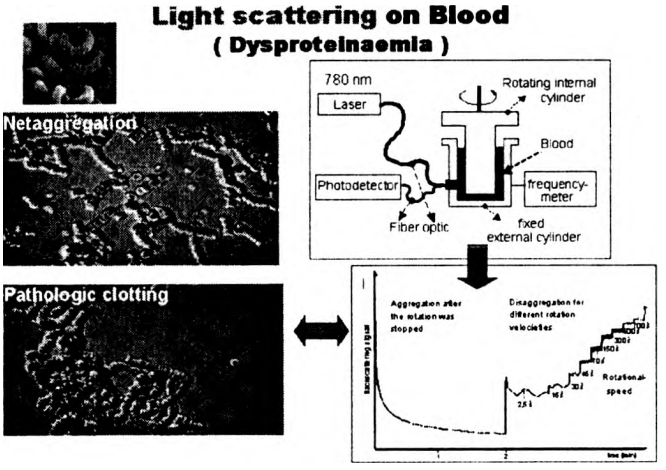

Fig. 17. Aggregation of red blood cells on different stages, including the set-up of the aggregometer.

disaggregation behaviour. Light scattering measurements were used for the investigation of the changes of shear forces [41]. The blood sample is placed into a gap between a rotating internal cylinder and a stationary outer cylinder. The radiation of a He-Ne laser or a red laser diode is used for the measurement. A single wave guide is used for the illumination, whereas four fiber-optic sensors are used for transmitting the backscattered light to the detector. However, the alteration of the intensity of the backscattered light and consequently of the photocurrent, time-related to the aggregation kinetics by change of the shear force, is recorded (Fig. 17).

Diabetes was selected for initial clinical investigations because it can be evaluated by established methods using blood samples. While aggregation kinetics show only slight differences in diabetic patients, disaggregation kinetics reveal significant

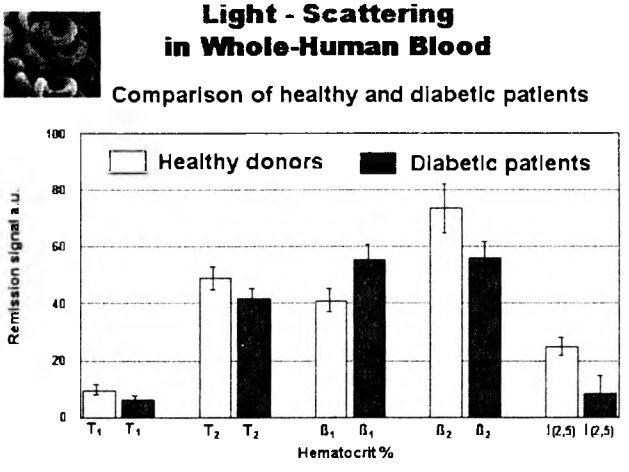

Fig. 18. Comparison of healthy and diabetic patients.

differences (Fig. 18). Blood samples were investigated for dysproteinaemias, too. The spectroscopically determined parameters of both aggregation and disaggregation kinetics were compared to the rheologic lab data. The spectroscopically determined parameters β_1 and β_2 turned out to significantly differ in patients with and those without dysproteinaemias. Consequently, the stability of the large aggregates is decisively higher in diabetic patients than that in healthy volunteers [42].

A major concern in biotechnology is the controlled reproduction and fermentation processes of cell cultures in nutrient solution. This means that the cell reproduction process inside a totally enclosed bioreactor should be monitored. Cell concentration increases during the biotechnological process and a gradual change in colour of the nutrient solution and the scattering and absorption behaviour of the reactor material can also be observed. The Biocheck measuring set-up was developed in order to monitor and control the quality of turbid media (milk, cell suspensions, *etc.*). A miniaturized double Ulbricht sphere measuring set-up was realized for this purpose. The basic idea was to use a suitable function to characterize the scattering behaviour of particles in a fluid illuminated by monochromatic laser light. The spectral absorption coefficient μ_a

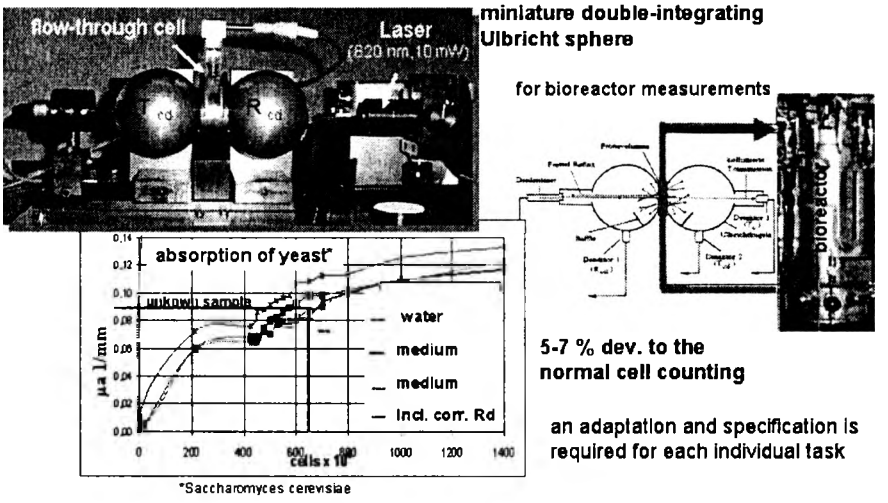

Fig. 19. Picture of the prototype Biocheck, which is used for the measurement of turbid fluids.

at 820 nm was considered to be a suitable parameter for this purpose. The use of coefficient μ_a as a quality feature offers the advantage that only remission and transmission must be recorded as measuring data. As a consequence the function course of μ_a is dependent on the specimen quality–cell quantity. A layer thickness of 1 cm was used. In order to determine the measuring accuracy of the experimental set -up, standard curves of cell suspensions (yeast cells) with known cell densities were recorded in a primary step (Fig. 19). Commercial full-cream milk (3.5 vol % fat content) was used to test the experimental set-up. Such a sensor system may prove useful no only for foodstuff control, but also for future applications in the field of medical biotechnology.

2.2.4. Biogene gases

Another important topic in biomedicine and clinics belongs to the sensitive and fast detection of biogene gaseous compounds. The use of lasers in medical applications has grown enormously in the last few years. During the surgical procedures the thermal destruction of tissue generates a smoke plume. Recent chemical analysis of the laser as well as electrosurgery pyrolysis product revealed that aerosols or gaseous compounds generated by pyrolytic decomposition of tissue may lead to health hazards [43]. In view of the cancerogenic and mutagenic potential of the laser aerosol (particles), pyrolytic products might also possess infectious as well as toxic properties.

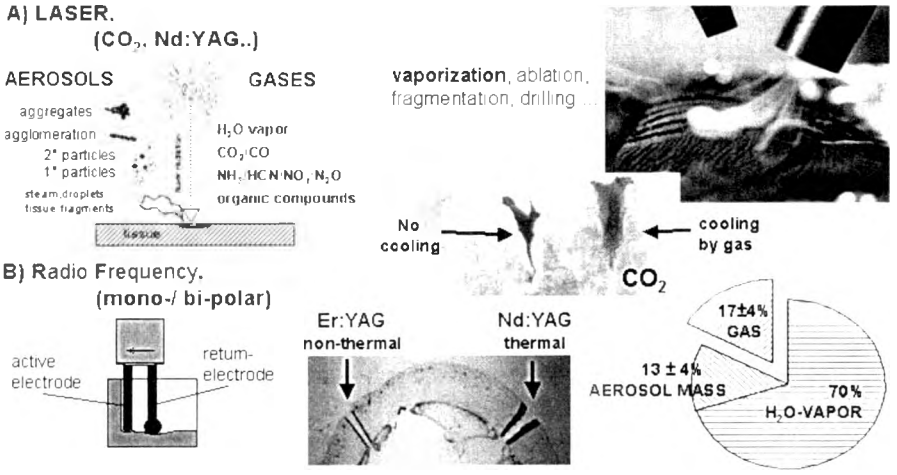

Fig. 20. Scheme for laser- and electrosurgery. Photographs due to the thermal affects on laser–tissue interaction are shown.

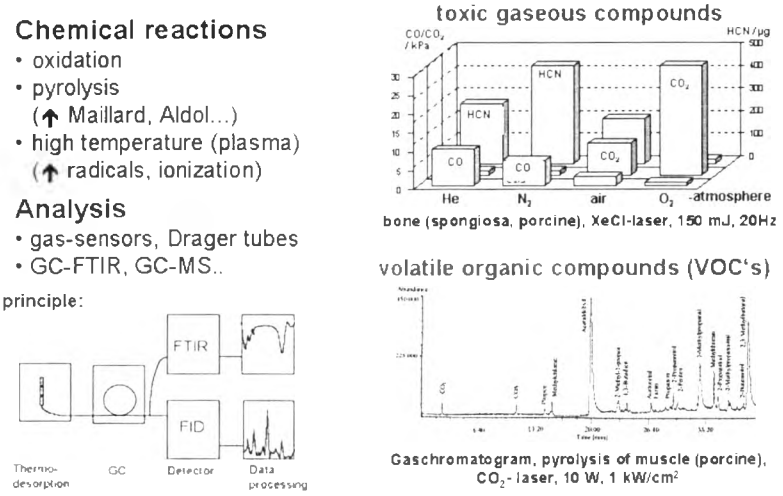

Fig. 21. Results of the laser plume composition.

However, by varying the process parameters, the composition of the mixture of low molecular gases and volatile organic components (VOC) was investigated by optical methods. A coupled system of gas chromatography and infrared spectroscopy (was used to separate the laser plume mixture, in order to detect and analyze the major compounds inside the laser smoke (Figs. 20, 21). The aerosols were investigated using IR spectroscopy (ATR mode) too.

2.3. Raman spectroscopy

For the analysis of volatile gases due to metabolic pollutants a multichannel Raman sensor for monitoring purposes was developed [44]–[46]. Subject of the investigation was the quantitative analysis of gases using linear vibrational Raman scattering technologies. In Figure 22 a setup for the simultaneous detection of up to 6 gases in the ppb and ppt domain is shown. Linear vibrational Raman scattering is often used for analysis of bi- and multiple atomic molecules. The scattering cross-section obtained was normalized to the nitrogen molecule. The experimental set-up realized is mobile and has additional advantage, *e.g.*, optical measurement basis, compactness, *etc.*

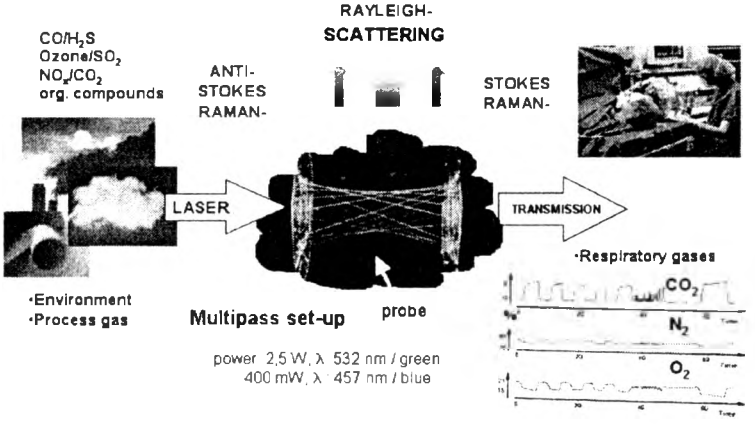

Fig. 22. Technical set-up for the multipass Raman sensor.

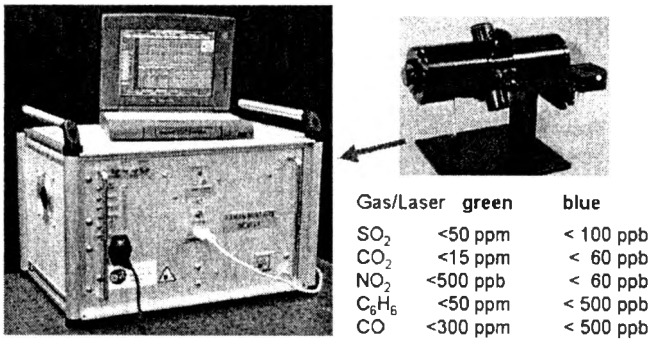

Gas/Laser	green	blue
SO_2	<50 ppm	< 100 ppb
CO_2	<15 ppm	< 60 ppb
NO_2	<500 ppb	< 60 ppb
C_6H_6	<50 ppm	< 500 ppb
CO	<300 ppm	< 500 ppb

Fig. 23. Photograph of the multipass Raman sensor prototype and the detection limits of selected gases.

To detect Raman scattering radiation for quantitative analysis of the composition of gaseous compounds, the gas molecules are irradiated by a narrow-band light source. Like a fingerprint for each kind of molecule, the bathochromically shifted Raman scattering is detected. The scattering intensity within the detector volume can be converted into a concentration.

The relatively low efficiency of the Raman scattering can be compensated by optimizing the transmission properties of all optical components used and by multipass radiation through the transparent gas sample. Diode-pumped solid-state lasers with internal frequency doubling are used as light sources. For spectral dissociation of the stray light combined interference filters are employed. The comparison between green (532 nm) and blue (457 nm) excitation indicates a distinct increase in the detection sensibility in favour of the blue excitation (Fig. 23).

3. Non-optical methods

A range of spectroscopic procedures is used for the detection of dangerous gaseous compounds. The measurement of trace amounts of toxic gases and vapours is of major interest for pollutant monitoring, particularly in industry and ecology. Currently, ion mobility spectrometry (IMS) is the only detection method which is capable of reliably recognizing a specific molecule among 10^9 other ones (ppt range). If charged molecules enter an electrical field at normal pressure, they drift towards a collecting electrode in the direction of the field. All ions differ by mass and collision frequency and it is these properties which influence their mobility. This means that different ions reach the collector at different intervals after having drifted inside the electrical field and allows the ions to be identified. The illustration shows a diagrammatic view of an ion drift sensor. In the ion source the molecules are ionized by charge transfer from the cluster ions that are permanently there. Periodically, a grid opens the drift room,

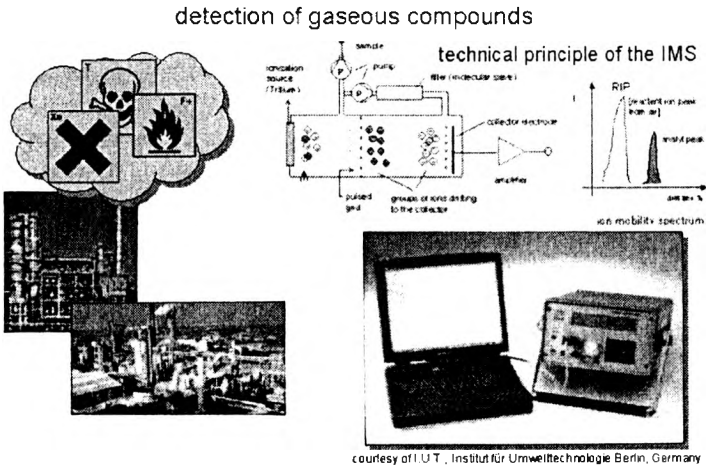

Fig. 24. Technical principle of the ion mobility spectrometry.

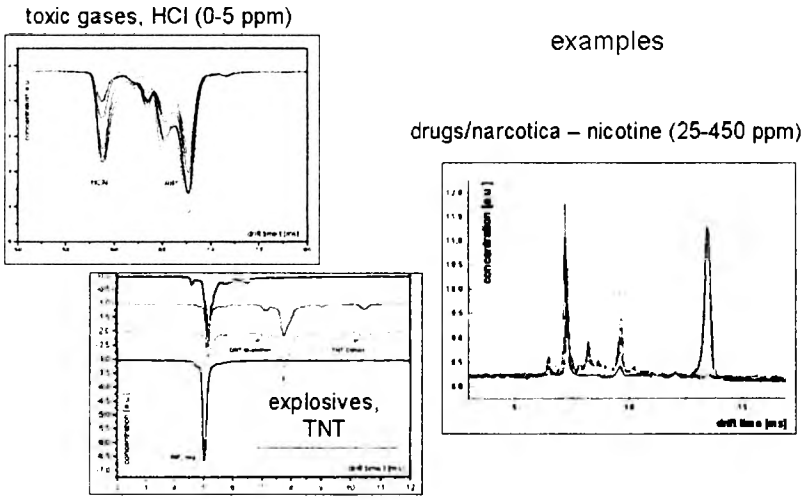

Fig. 25. Current IMS applications for a sensitive determination of contaminates are given.

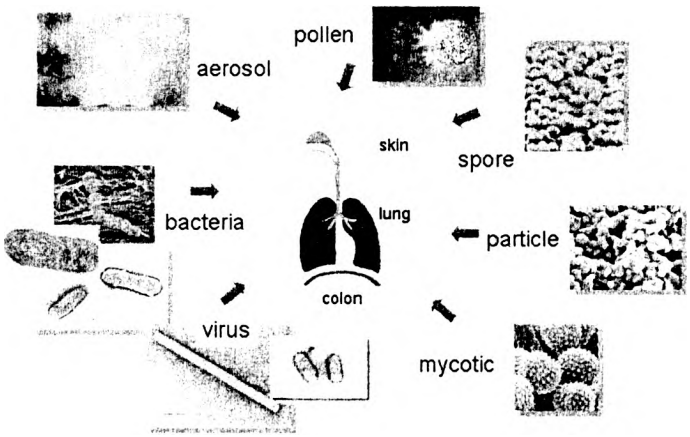

Fig. 26. Environmental stress of the human body caused by organic and inorganic particles.

in which the ion compound is separated. The ions reach the collector at different intervals and form the drift spectrum (Fig. 24). Figure 25 shows the measuring results for various applications.

The IMS device is easily transported and can be adapted for any specific application. Depending on the assignment, it may be necessary to modify the device in terms of sample loading or pre-separation. It is a generally accepted fact in the medical field that the composition of exhaled air and transpiration relates to the patient's state of health. A well-known example is the increased ketone content of exhaled air in the case of those suffering from diabetes, this being due to metabolic changes. In addition to such pathologic changes, the organism is constantly subjected to organic and inorganic particle stress (Fig. 26).

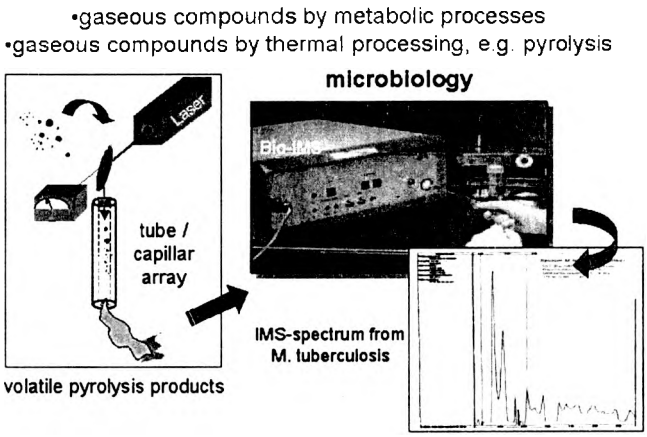

Fig. 27. Scheme of the laboratory set-up for the detection of specific volatiles after laser pyrolysis.

For specific treatment, early detection together with fast and reliable identification of bacterial infections is of primary importance in medicine. Laser- und Medizin -Technologie GmbH, Berlin, TB is currently participating in an international project, the subject of which is the early detection of tuberculosis. While one approach concentrates on detection of a specific volatile signature within the metabolism (as single compound and as signal pattern), it is also possible to use laser pyrolytic procedures as shown in Fig. 27 to generate such a signature. This can be explained by the different biochemical and molecular biological structure of bacterial cell walls (Fig. 28).

Such procedures may be analogously applied to problems arising in biotechnology, *i.e.*, for quality and process control, quality assurance in agricultural sciences and

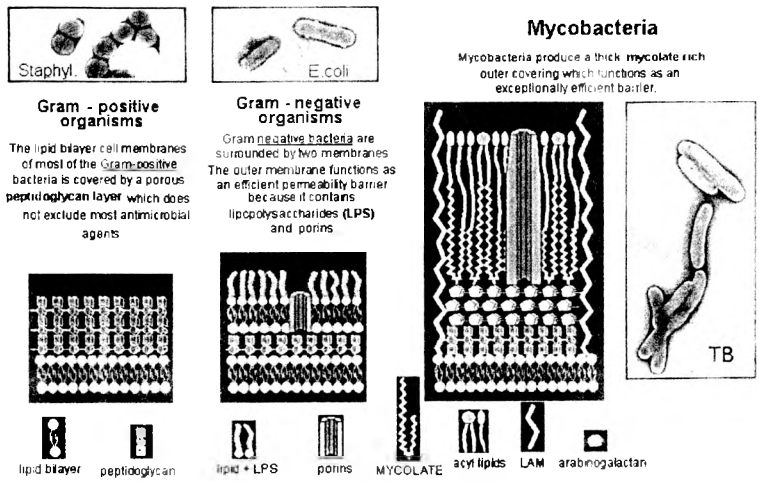

Fig. 28. Schematic composition of the bacterial cell membranes (Gram-positive, Gram-negative and mycobacteria).

veterinary medicine as such problems are not limited to gaseous and volatile biogenetic compounds (odor sensor analysis). Initial joint investigations have been prepared for microcapillary arrays which when coated by sol-gel, doped with ruthenium -tris(bipyridinium), could be used as surface-modified elements for laser induced pyrolysis (Fig. 29) or simultaneously for an optical reference detection method [47], [48].

To ensure that different mycobacteria (tuberculosis, avium, szugali, *etc.*) can be distinguished from one another, preliminary investigations considered the growth periods of different cultures and species were carried out. For those investigations a MALDI system was used (Fig. 30). Compared to IMS, up to now MALDI systems are

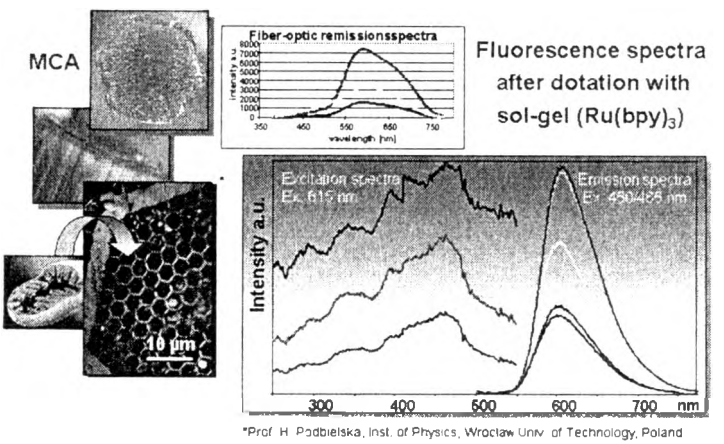

Fig. 29. Picture of a microcapillar array, before and after sol-gel coating. The sol-gel was doped by $Ru(bpy)_3$, fiber-optic remission- and fluorescence spectra were recorded.

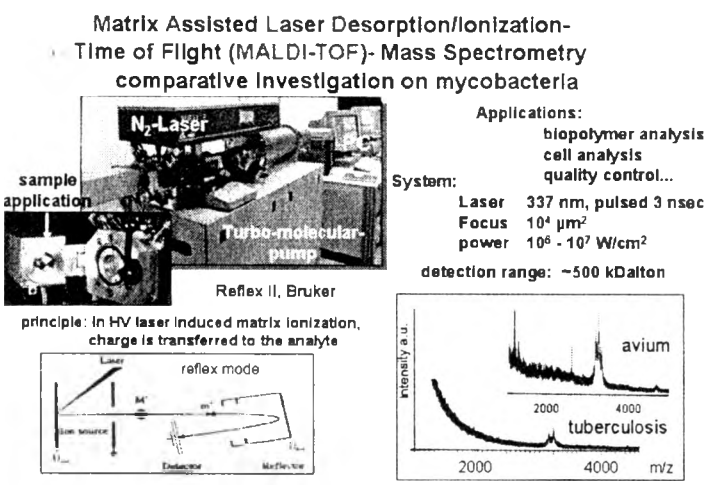

Fig. 30. MALDI mass spectrometry for the determination of characteristic signal pattern of intact mycobacteria.

very expensive, complex, large-size units which are unsuitable for use in daily routine. They are, however, indispensable for various quality control applications in material sciences and for purposes of proteomics and others [49]–[57].

4. Conclusion

This article presents a selection of laser supported spectroscopic techniques together with examples of relevant areas of use in medicine, agriculture/food and biotechnology of the present day. Solid, liquid and gaseous bio-samples are the subjects of interest. The development of robust, optical devices for simple, rapid and safe analytical measurements remains the central task for non-invasive or minimally invasive diagnostics in biomedicine and associated fields. This is why implementation of novel materials such as Sol-gel technology for fibre optic use as well as the arrangement of highly sensitive IMS-technique and effective laser pyrolysis, may be a promising outlook for new innovative optical sensors in the future.

References

[1] VERDAASDONK R.M., VAN SWOL C.F.P., Phys. Med. Biol. **42** (1997), 869.
[2] WÄSCHE W., BINDIG U., MÜLLER G., FREGE P., GROSS U.M., Proc. SPIE **3197** (1998), 86.
[3] LASCH P., WÄSCHE W., BINDIG B., NAUMANN D., MÜLLER G., *ibidem*, 278.
[4] MÜLLER G., WÄSCHE W., LIEBOLD K., BINDIG U., Laser Phys. **9** (1999), 348.
[5] BINDIG U., WÄSCHE W., LIEBOLD K., WINTER H., KNAPPE V., MÜLLER G., GROSS U.M., FREGE P., Proc. SPIE **3568** (1999), 38.
[6] GERSONDE I.H., MEINKE M., BECKER Y., BINDIG U., EPPICH B., MÜLLER G., Proc. SPIE **3920** (2000), 86.
[7] DIEM M., BOYDSTON-WHITE S., CHIRIBOGA L., Appl. Spectrosc. **53** (1999), 148A.
[8] JACKSON M., KIM K., TETTEH J., MANSFIELD J.R., DOLENKO B., SOMORJAI R.L., ORT F.W., WATSON P.H., MANTSCH H.H., Proc. SPIE **3257** (1998), 24.
[9] HOCDÉ S., BOUSSARD-PLÉDEL C., FONTENEAU G., LUCAS J., Solid State Sci. **3** (2001), 279.
[10] SCRIPACHEV I.V., CHURBANOV M.F., DEVYATYKH G.G., DIANOV E.M., PLOTNICHENKO V.G., Proc. SPIE 2002, in press.
[11] FRANK J., SCHINDLER R., LENDL O., LENDL B., Appl. Spectrosc. **54** (2000), 1417.
[12] KÜPPER L., HEISE H.M., BECHARA F.-G., STÜCKER M., J. Mol. Struct. **565-566** (2001), 497.
[13] BINDIG U., MEINKE M., GERSONDE I., SPECTOR O., VASSERMAN I., KATZIR A., MÜLLER G., Sens. Actuators B **74** (2001), 37.
[14] KÜPPER L., HEISE H.M., BUTVINA L.N., J. Mol. Struct. **563-564** (2002), 173.
[15] HOCDE S., LOREAL O., SIRE O., TURLIN B., BOUSSARD-PLEDEL C., LE COQ D., BUREAU B., FONTENEAU G., PIGEON C., LEROYER P., LUCAS J., Proc. SPIE **4158** (2001), 49.
[16] UEMURA T., NISHIDA K., SAKAKIDA M., ICHINOSE K., SHIMODA S., SHICHIRI M., Front. Med. Biol. Eng. **9** (1999), 137.
[17] BORMASHENKO E., POGREB R., SUTOVSKI S., LEVIN M., Opt. Eng. **41** (2002), 295.
[18] KERSLAKE E.D.S., WILSON C.G., Adv. Drug Delivery Rev. **21** (1996), 205.
[19] BAULSIR C.F., SIMLER R.J., *ibidem*, 191.
[20] ARTJUSHENKO V.G., AFANASYEVA N.I., LERMANN A., KRYUKOV A.P., KUZIN E.F., ZHARKOVA N.N., PLOTNICHENKO V.G., FRANK G.A., DIDENKO G.I., SOKOLOV V.V., NEUBERGER W., Proc. SPIE **2025** (1994), 137.
[21] GOTSHAL Y., SIMHI R., SELA B.-A., KATZIR A., Sens. Actuators B **42** (1997), 157.

[22] AFANASYEVA N.I., KOLYAKOV S., BUTVINA L.N., Proc. SPIE **3257** (1998), 260.
[23] BRUCH R.F., SUKUTA S., AFANASYEVA N.I., KOLYAKOV S.F., BUTVINA L.N., Proc. SPIE **2970** (1997), 408.
[24] BROOKS A., BRUCH R.F., AFANASYEVA N.I., KOLYAKOV S.F., BUTVINA L.N., MA L., Proc. SPIE **3262** (1998), 173.
[25] WU J.-G., XU Y.-Z., SUN C.-W., SOLOWAY R.D., XU D.-F., WU Q.-G., SUN K.-H., WENG S.-F., XU G.-X., Biopolymers **62** (2001), 185.
[26] WENG S.-F., LING X.-F., SONG Y.-Y., XU Y.-Z., LI W.-I., ZHANG X., YANG L., SUN W., ZHOU X., WU J., Am. Clin. Lab. **19** (2000), 20.
[27] BUNIMOVICH D., KELLNER R., KRSKA R., MESICA A., PAISS I., SCHIESL U., TACKE M., TAGA K., KATZIR A., J. Mol. Struct. **292** (1993), 125.
[28] WERLE P., SLEMR F., MAURER K., KORMANN R., MÜCKE R., JÄNKER B., Opt. Lasers Eng. **37** (2002), 101.
[29] BINDIG U., MEINKE M., GERSONDE I.H., SPECTOR O., KATZIR A., MUELLER G., Proc. SPIE **4129** (2000), 249.
[30] BEUTHAN J., BOCHER T., MINET O., ROGGAN A., SCHMITT I., WEBER A., MÜLLER G., Proc. SPIE **2135** (1994), 147.
[31] BOCHER T., BEUTHAN J., SCHELLER M., HOPF J., LINNARZ M., NABER R., MINET O., BECKER W., MÜLLER G., Proc. SPIE **2627** (1995), 118.
[32] HELFMANN J., SCHÜTZ R., MÜLLER G.J., Minimal Invasive Medizin **7** (1996), 172.
[33] BOCHER T., LUHMANN T., BAIER S., DIEROLF M., NAUMANN M., BEUTHAN J., BERLIEN H.-P., MÜLLER G., Proc. SPIE **3197** (1997), 60.
[34] CHAN S., FAUCHET P.M., LI Y., ROTHBERG L.J., Proc. SPIE **3912** (2000), 23.
[35] CHAN S., HORNER S.R., FAUCHET P.M., MILLER B.L., J. Am. Chem. Soc. **123** (2001), 11797.
[36] GLOTZ M., HUG B., SCHOLZ C., MÜLLER G.J., ROGGAN A., KNAPPE V., MESECKE-VON-RHEINBABEN I., Proc. SPIE **3193** (1998), 60.
[37] RITZ J.-P., ROGGAN A., GERMER C.T., ALBRECHT D., BUHR H.J., *Bestimmung der optischen Parameter von humanem Lebergewebe und Lebermetastasen zur Bestrahlungsplanung bei laserinduzierter Thermotherapie von Lebermetastasen*, Langenbecks Arch. Chir. I (Forumband 1997), 1997, pp. 335–8.
[38] RITZ J.-P., ROGGAN A., ISBERT C.M., ALBRECHT D., GERMER C.T., MÜLLER G.J., BUHR H.J., Proc. SPIE **3193** (1998), 80.
[39] ROGGAN A., FRIEBEL M., DOERSCHEL K., HAHN A., MUELLER G.J., Proc. SPIE **3195** (1998), 51.
[40] ROGGAN A., FRIEBEL M., DÖRSCHEL K., HAHN A., MÜLLER G., J. Biomed. Opt. **4** (1999), 36.
[41] LADEMANN J., WEIGMANN H.-J., STERRY W., ROGGAN A., MÜLLER G., PRIEZZHEV A.V., FIRSOV N.N., Laser Phys. **9** (1999), 357.
[42] PRIEZZHEV A.V., RYABOSHAPKA O.M., FIRSOV N.N., SIRKO I.V., J. Biomed. Opt. **4** (1999), 76.
[43] WÄSCHE W., WAGNER G., ALBRECHT H., MÜLLER G., Minimal Invasive Medizin **4** (1993), 35.
[44] ALBRECHT H., *Clinical and Respiratory Gas Analysis, in Sensors: A Comprehensive Survey*, [Eds.] Göpel W., Hesse J., Zemel J.N., Part 2, Vol. 3, Chap. 23, pp. 1049–93, VCH 1991.
[45] ALBRECHT H., WINTER H., WÄSCHE W., Fortschr. Lasermed. **12** (1995), 154.
[46] HERRIG M., WINTER H., *ibidem*, 155.
[47] ANDRZEJEWSKI D., PODBIELSKA H., ULATOWSKA A., Opt. Appl. **4** (2000), 503.
[48] LECHNA M., HOLOWACZ I., ULATOWSKA A., PODBIELSKA H., Surf. Coat. Technol. **151-152** (2002), 299.
[49] SULTANA S., MAGEE J.T., DUERDEN B.I., Clinical Infectious Diseases, Suppl., **20** (1995), 122.
[50] CLAYDON M.A., DAVEY S.N., EDWARDS-JONES V., GORDON D.B., Nature Biotechnology **14** (1996), 1584.
[51] BASILE F., BEVERLY M.B., VOORHEES K.J., HADFIELD T.L., Trends in Analytical Chemistry **17** (1998), 95.
[52] FREEMAN R., GOODACRE R., SISSION P.R., MAGEE J.G., WARD A.C., LIGHTFOOT N.F., J. Medical Microbiology **40** (1999), 170.

[53] VAN BAAR B.L.M., FEMS Microbiology Rev. **24** (2000), 193.
[54] LAY J.O., Trends in Analytical Chemistry **19** (2000), 507.
[55] FUERSTENAU S.D., BENNER W.H., THOMAS J.J., BRUGIDOU C., BOTHNER B., SIUZDAK G., Angewandte Chemie **113** (2000), 559.
[56] CHACE D.H., Chem. Rev. **101** (2001), 445.
[57] JUNGBLUT P.R., Microbes and Infection **3** (2001), 831.

Received October 4, 2002